ISSN 2462-2052 | eISSN 2600-8718 *Journal of Science and Mathematics Letters*
DOI: https://doi.org/10.37134/jsml.vol13.2.5.2025 *Volume 13, Issue 2, 57-71, 2025*

Research Article

Phytochemical Influence of *Scutellaria iscanderi* L. on Zinc Oxide Nanoparticle Biosynthesis

Shamansur Sagdullayev[1], Iroda Shermatova[2]*, Azizakhon Khusniddinova[2], Dilobar Tayirova[2] and Zakirova Rukhsona[2]

[1]S.Y. Yunusov Institute of the Chemistry of Plant Substances, Academy of Sciences of Uzbekistan, Tashkent 100170, Uzbekistan
[2]Tashkent Pharmaceutical Institute, Tashkent 100015, Uzbekistan
*Corresponding author: iroda.shermatova.94@mail.ru

Received: 9 June 2025; **Accepted:** 20 August 2025; **Published:** 25 August 2025

ABSTRACT

The rapid development of nanotechnology requires environmentally friendly and biocompatible approaches for the synthesis of nanomaterials with stable physicochemical properties. Green synthesis using plant extracts provides a sustainable alternative due to their natural biomolecules that initiate and regulate nanoparticle formation. This study aimed to synthesize zinc oxide nanoparticles (ZnO-NPs) using the extract of *Scutellaria iscanderi* L. and to investigate the role of its phytochemical components in nanoparticle formation and stabilization. ZnO-NPs were synthesized via a biogenic route employing the aqueous extract of S. iscanderi. The influence of amino acids, carbohydrates, and flavonoids in reduction and stabilization was evaluated, and the obtained nanoparticles were characterized using modern analytical techniques. Amino acids and carbohydrates facilitated nanoparticle reduction and controlled growth, while flavonoids acted as natural stabilizers, preventing aggregation and providing antioxidant protection. Characterization confirmed the formation of stable ZnO-NPs with desirable physicochemical properties. The extract of *S. iscanderi* effectively mediated the green synthesis of ZnO-NPs through the synergistic action of its biomolecules. These findings highlight the potential of *S. iscanderi*-derived nanoparticles for applications in pharmaceutical, medical, and environmental fields.

Keywords: Zinc oxide nanoparticles (ZnO-NPs), green synthesis, *Scutellaria iscanderi*, amino acids, carbohydrates, flavonoids

1. INTRODUCTION

Metal nanoparticles and their oxides, particularly zinc oxide (ZnO), represent a class of materials with unique physicochemical properties determined by their nanoscale nature. These properties include high specific surface area, photocatalytic activity, pronounced antibacterial effects, and biocompatible interactions with cells and tissues (Azam et al., 2021; Javed et al., 2020). As a result, ZnO-based nanomaterials have found wide application across diverse fields from pharmaceuticals, medicine, and cosmetics to the food industry and environmental protection (Khan et al., 2020). Although conventional physicochemical synthesis methods, such as precipitation, microwave-assisted techniques, ultrasonic treatment, and sol-gel

processes, enable the production of nanostructures with well-defined parameters, they are associated with several significant limitations. These include the high cost of equipment, the necessity for aggressive chemical reagents and solvents, and the environmental risks associated with toxic by products, which undermine their sustainability in the context of green chemistry principles (Rajiv et al., 2013). Consequently, recent years have witnessed growing interest in developing alternative, environmentally friendly approaches to nanoparticle synthesis especially green or biogenic methods. These approaches rely on biological agents such as bacteria, fungi, algae, yeasts, and particularly higher plants, which are capable of reducing metal ions to nanoparticles through the action of their intrinsic biomolecules, including proteins, enzymes, sugars, flavonoids, phenolic compounds, and other natural metabolites (Ramesh et al., 2015; Singh et al., 2022). Among the most promising directions in green nanotechnology is biosynthesis the fabrication of nanoparticles using aqueous or alcoholic plant extracts. This method offers several undeniable advantages, including the availability and renewability of plant materials, process safety, environmental sustainability, scalability, and the ability to modulate the morphological and functional properties of the resulting nanoproducts (Lithi et al., 2025). Studies by Al-Darwesh et al. have shown that ZnO-NPs synthesized using biochemically active substances exhibit enhanced stability, narrow particle size distribution, and improved functional properties, making them particularly attractive for biomedical applications (Al-Darwesh et al., 2024).

The present study focuses on the development and optimization of a green synthesis method for ZnO-NPs using an aqueous extract of *S. iscanderi* a medicinal plant rich in flavonoids, carbohydrates, and proteins that play a key role in the reduction and stabilization of nanostructures. Special attention is given to the influence of synthesis parameters such as temperature, pH, and molar ratio of reagents on the rate of nanoparticle formation, their morphological characteristics, and their potential biomedical relevance.

2. MATERIALS AND METHODS

2.1. Preparation of Plant Extract and Optimization of Flavonoid Extraction

The aerial parts of *S. iscanderi* were systematically harvested during their peak vegetative phase in July from the Pap district of Namangan region, Uzbekistan (Draft Pharmacopoeial Monograph (DPM) 42 Uz-15842845-3731-2019) (Shermatova and Rizayev, 2025). The collected plant material was thoroughly rinsed with distilled water to remove impurities, shade-dried for 7 days at ambient temperature to preserve thermolabile phytoconstituents, and finely ground using a stainless-steel mechanical grinder. For aqueous extraction, precisely 10 g of powdered sample were mixed with 80 mL of distilled water, maintaining a hydromodule of 1:8. The mixtures were subjected to thermal extraction at three controlled temperatures 30°C, 50°C and 70°C for 60 min under continuous magnetic stirring to evaluate the temperature-dependent efficiency of flavonoid release. Post-extraction, the suspensions were filtered using filter paper and the filtrates were stored at 4°C in amber vials to prevent photodegradation.

The flavonoid concentrations in the resulting extracts were quantified using high-performance liquid chromatography (HPLC) to determine the optimal extraction condition. The effect of temperature on flavonoid extraction in the aqueous extract of *S. iscanderi* is presented in Table 1. As evident from the presented data, the maximum extraction of apigenin, quercetin, rutin, and luteolin in the aqueous extract was observed at 70°C.

Table 1. Effect of extraction temperature on the yield of various flavonoids

Flavonoids	Effect of Temperature on Flavonoid Content in Aqueous Extract (hydromodule 1:8)		
	30°C	50°C	70°C
	Flavonoid Content in Aqueous Extract of *S. iscanderi* (mg/g)		
Apigenin	0.157080	0.327080	0.372080
Quercetin	0.050557	0.013557	0.146870
Rutin	0.155127	0.227127	0.242126
Luteolin	0.120709	0.130709	0.133604

2.2. Biosynthesis of ZnO-NPs via the Green Synthesis Method

The biosynthesis of ZnO-NPs was carried out using an extract of *S. iscanderi* a plant rich in biologically active compounds particularly flavonoids which function as natural reducing and stabilizing agents. These bioochemicals facilitate the efficient reduction of zinc ions and promote the formation of nanoparticles with controlled size and morphology. An aqueous 0.5 M solution of zinc acetate dihydrate [$Zn(CH_3COO)_2•2H_2O$] served as the precursor for zinc ion provision. The freshly prepared aqueous plant extract was introduced into the precursor solution in a controlled, dropwise manner under continuous magnetic stirring at ambient temperature. This controlled addition ensured homogeneous mixing and promoted a gradual and uniform nucleation process. To systematically assess the influence of extract-to-precursor volume ratios on the kinetics, yield, and efficiency of nanoparticle formation, a range of compositional ratios was investigated, as summarized in Table 2. The synthesis of ZnO-NPs was conducted using the green synthesis method, with the stages of the process illustrated in Figure 1.

Table 2. Effect of temperature and extract ratio on the formation of ZnO-NPs

Ratio of Extract (obtained at 50°C) + Zinc Acetate Dihydrate	Onset of Color Change (Start of Biosynthesis) at t = 30 °C	Time When Color Change Ceased	Ratio of Extract (obtained at 70°C) + Zinc Acetate Dihydrate	Onset of Color Change (Start of Biosynthesis) at t = 50°C	Time When Color Change Ceased
1:1	15 min	40 min	1:1	8 min	38 min
1:2	17 min	45 min	1:2	10 min	42 min
1:3	20 min	50 min	1:3	10 min	48 min
1:4	23 min	55 min	1:4	11 min	53 min
1:5	26 min	60 min	1:5	12 min	58 min
1:10	29 min	65 min	1:10	14 min	60 min
2:1	15 min	70 min	2:1	9 min	62 min
2:2	18 min	75 min	2:2	12 min	73 min
3:2	13 min	65 min	3:2	6 min	35 min
3:5	15 min	62 min	3:5	9 min	40 min

A series of reaction suspensions was subsequently formulated by combining the aqueous extract of *S. iscanderi* with a 0.5 M solution of zinc acetate dihydrate in systematically varied volume ratios. The initial pH of all reaction mixtures was measured at approximately 6. To trigger the precipitation and initiate nanoparticle formation, 15 mL of 2 M NaOH solution was carefully introduced into each system. This addition led to the immediate development of a dense colloidal matrix, indicating the onset of nucleation and subsequent growth of ZnO-NPs. During the biosynthesis process, a gradual color change of the reaction mixture was observed at different time intervals, depending on the reaction conditions. The results indicate that both the extract-to-precursor ratio and the synthesis temperature significantly influence the nature and rate of color transition. At 50°C, the onset of visible color change was recorded after 6 min and persisted until the 35 minute. The transformation of the suspension color from white to

deep yellow is indicative of an increasing concentration and growth in size of the forming ZnO-NPs.

Figure 1. External appearance of the studied material, raw plant material and extract

The most pronounced nanoparticle formation was observed at an extract-to-zinc acetate ratio of 3:2 suggesting this as the optimal composition under the given experimental conditions. In addition to the reagent ratio, synthesis temperature and reaction medium pH were found to play critical roles in determining the kinetics of nanoparticle formation. Across all tested samples, the pH remained within the range of 6.0-7.2 and was stable throughout the reaction duration. An increase in synthesis temperature significantly accelerated nanoparticle formation. At a 3:2 ratio, the onset of biosynthesis occurred after 13 min at 30°C, whereas at 50°C, it was reduced to 7 min. Similarly, the completion of color change which serves as an indirect indicator of synthesis completion was observed 30 min earlier at 50°C (35 min), compared to 65 min at 30°C. Thus, it can be concluded that the most favorable conditions for the green synthesis of ZnO-NPs are a temperature of 50°C and an extract-to-precursor ratio of 3:2, which together ensure the highest rate and efficiency of nanoparticle formation.

2.3. Spectroscopic and Chromatographic Characterization

Fourier-Transform Infrared (FTIR) spectroscopy was used to identify functional groups in the *S. iscanderi* extract and to monitor chemical changes after ZnO-NP biosynthesis. Spectra were recorded in the range of 4000-400 cm^{-1} and the observed vibrations confirmed the involvement of plant biomolecules in nanoparticle reduction and stabilization. UV-Vis spectroscopy was applied to confirm and characterize the formation of ZnO-NPs synthesized using the aqueous extract of *S. iscanderi*. The absorption spectra were recorded in the wavelength range of 200-800 nm, covering both the ultraviolet and visible regions where characteristic bands of ZnO nanostructures and plant-derived biomolecules typically appear. The detection of a distinct absorption peak verified the successful synthesis of ZnO-NPs and provided insights into their optical behavior and colloidal stability, in agreement with previous green synthesis reports (Akşit and Gergin, 2025).

The flavonoid content of *S. iscanderi* was determined by HPLC with UV detection using a C18 column. Methanolic solutions of plant extracts and standard reference compounds were filtered and analyzed under optimized conditions. Chromatographic separation was performed at room temperature with a mobile phase composed of Solutions A and B, at a flow rate of 1.0 mL/min and an injection volume of 10 µL. The total run time was 15-20 min. Identification and quantification were carried out by comparing retention times and peak areas of analytes with those of the corresponding standards with adequate chromatographic resolution achieved. Before quantitative determination, the suitability of the HPLC system was verified using at least five replicate injections of the standard reference solution of the target flavonoid. The system was considered acceptable when column efficiency (N) exceeded 2000, the resolution

(Rs) between adjacent peaks was ≥1.5, and the relative standard deviation (RSD) of peak areas did not exceed 2.0%. Quantification was performed by comparing the chromatographic response of the analyte in the test solution with that of the standard solution, using the following equation:

$$X = \frac{S_{test} \times a_{std} \times V_{test} \times P \times 1000}{S_{test} \times V_{std} \times a_{test} \times 100} = \frac{S_{test} \times a_{std} \times P \times V_{test} \times 10}{S_{std} \times a_{test} \times V_{std}}$$

where S_{test} represents the peak area of the test solution, S_{std} the peak area of the standard solution, a_{std} the weight of the standard sample in grams, a_{test} the weight of the test sample in grams, P the percentage content of the reference substance in the standard sample, V_{std} the volume of dilution of the standard solution (mL), V_{test} the volume of dilution of the test solution (mL), and X the percentage content of the analyte in the sample.

For the quantitative analysis of apigenin, quercetin, rutin, and luteolin, weighed portions of the powdered sample were dissolved in methanol, diluted to 100 mL and filtered through blue-ribbon paper. Chromatographic separation was performed on a reversed-phase C18 column with a flow rate of 1.0 mL/min and total analysis time of 20 min. UV detection was carried out at compound-specific wavelengths, and the content of each flavonoid (%) was calculated according to the general HPLC formula. Reference standards (1.0 mg/mL in methanol) were used for calibration. According to the State Pharmacopoeia of the Republic of Uzbekistan, the content of flavonoids must not be lower than the prescribed minimum values.

Apigenin: λ = 335 nm; mobile phase: methanol; 0.3% trifluoroacetic acid (40:60, v/v); retention time ≈15 min; minimum content ≥0.20%; Quercetin: λ = 370 nm; mobile phase: methanol; 0.3% trifluoroacetic acid (20:80, v/v); retention time confirmed; minimum content ≥0.05%; Rutin: λ = 357 nm; mobile phase: methanol; 0.3% trifluoroacetic acid (20:80, v/v); retention time confirmed; minimum content ≥0.04%; Luteolin: λ = 350 nm; mobile phase: acetonitrile; 0.2% trifluoroacetic acid (28:72, v/v); retention time confirmed; minimum content ≥0.05%.

2.4. HPLC Method for the Quantitative Determination of Mono- and Disaccharides in Plant Extracts

Quantitative analysis of glucose, fructose, sucrose, and maltose in the samples was performed using an Agilent 1100 HPLC system (Agilent Technologies, USA) equipped with a refractive index detector. Separation was achieved on a Supelcosil LC-NH_2 column (5 µm, 4.6×250 mm; Supelco, USA) with isocratic elution using acetonitrile-water (82:18, v/v) as the mobile phase at a flow rate of 1.0 mL/min, column temperature 35°C, and injection volume 10 µL. Certified reference standards of the target carbohydrates were used for identification and calibration. Retention times were as follows: fructose 4.9±0.2 min, glucose 5.7±0.2 min, sucrose 10.4±0.2 min, maltose 12.1 ± 0.2 min. All solutions were prepared with deionized water and filtered through 0.45 µm nylon membranes before injection. The obtained chromatograms demonstrated baseline separation and reproducibility.

2.5. Methodology for the Isolation and HPLC Identification of Free Amino Acids in Aqueous Plant Extracts

Free amino acids from plant extracts were isolated by protein precipitation with 20% trichloroacetic acid (TCA). Equal volumes of extract and TCA solution were mixed, incubated for 10 min, and centrifuged at 8000 rpm for 15 min. The supernatant was collected, lyophilized, and neutralized by repeated dissolution in triethylamine:acetonitrile:water (1:7:1, v/v)

followed by evaporation to dryness. Derivatization was performed using phenyl isothiocyanate (PITC) to obtain phenylthiocarbamyl derivatives of amino acids. HPLC analysis was carried out on an Agilent 1200 Series system equipped with a diode-array detector and a Discovery HS C18 column (75 × 4.6 mm). Gradient elution was performed with eluent A (0.14 M sodium acetate with 0.05% triethylamine, pH 6.4) and eluent B (acetonitrile) at a flow rate of 1.2 mL/min. Detection was performed at 269 nm. The gradient program ranged from 1% to 60% B within 45 min, followed by re-equilibration. This method ensured reproducible separation and quantification of PTC-amino acids in complex plant matrices.

3. RESULTS AND DISCUSSION

3.1. FTIR Confirmation of ZnO-NPs Synthesis

FTIR spectroscopy was employed to confirm the formation of ZnO-NPs and to assess their quantitative features and optical properties. For the study, we used a ready-made suspension of ZnO-NPs obtained *via* green synthesis using *S. iscanderi.* The suspension was dried using lyophilization and used as the material for further analysis (Figure 2).

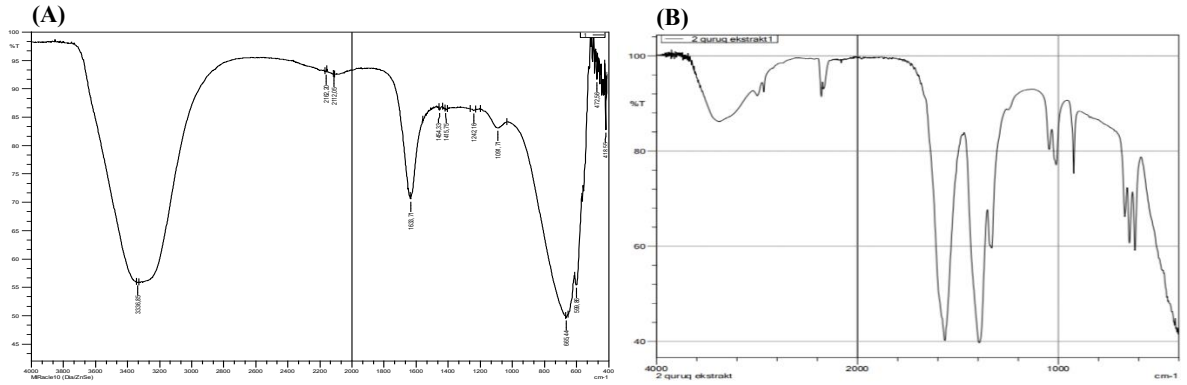

Figure 2. FTIR spectrum of the extract (**A**) and the substance containing ZnO-NPs (**B**)

In the spectrum, the following characteristic absorption regions can be identified: 1640-1560 cm^{-1}, 1055 cm^{-1}, 400-890 cm^{-1}, and the region around 3580 cm^{-1}. FTIR revealed a characteristic peak near 523 cm^{-1}, which indicated the formation of a ZnO nanostructure. The vibrational peaks observed around 3580 cm^{-1} correspond to hydroxyl (OH) groups. They appear as a narrow band in the spectra of diluted solutions in inert solvents or in the gas phase. When hydrogen bonding occurs, the vibration frequency decreases and the bands broaden. In some cases, both the free and hydrogen-bonded forms can be observed simultaneously. The recorded FTIR spectra indicated that the vibrational peaks at 1640 cm^{-1} and 1560 cm^{-1} corresponded to the bending vibrations of HOH groups. A broad absorption band in the region around 1750 cm^{-1} is present in the sample spectrum and relates to the stretching vibrations of OH groups in alcohols and phenolic compounds. Absorption bands in the range of 1055-870 cm^{-1} correspond to the stretching of COC groups in simple ethers and acetals. The absorption in the 400-890 cm^{-1} range characterizes various bonds in the pyranose ring, while the absorption band at 1640 cm^{-1} corresponds to pronounced carbonyl fragments of proteins. These results indicate that the carbonyl group of proteins is strongly adsorbed onto the metal surface. This suggests that proteins may also form a layer of bioorganic compounds facilitating interaction with the biosynthesized nanoparticles, while the secondary structure remains unaffected during the reaction with zinc ions or after binding with ZnO-NPs.

The aforementioned peaks confirm the presence of biochemicals in the plant extract, such as terpenoids and phenolic compounds, which were involved in the reduction and

stabilization of ZnO-NPs. The conducted experiments demonstrated that the studied sample contains ZnO-NPs. Using FTIR spectroscopy, it was demonstrated that plant metabolites such as sugars, terpenoids, polyphenols, alkaloids, phenolic acids, and proteins play a significant role in the reduction of metal ions into nanoparticles and in ensuring their subsequent stability. It was suggested that the control over size and morphology of the nanostructures may be associated with the interaction of these biomolecules with metal ions. After the addition of the plant extract to the precursor zinc acetate dihydrate and NaOH, a white precipitate was formed, indicating the phytoproduction of ZnO-NPs with a yield of 88.2%. This finding confirms the feasibility of large-scale production of ZnO-NPs using a plant-mediated synthesis procedure comparable to conventional chemical methods.

3.2. Evaluation of Optical Properties and Reducing Potential of S. iscanderi in ZnO-NPs Synthesis

The UV-visible spectral analysis provided clear evidence supporting the successful biosynthesis of ZnO-NPs using the aqueous extract of *S. iscanderi*. A pronounced and well-defined absorption peak was observed at approximately 370 nm, which is consistent with the characteristic surface plasmon resonance of ZnO-NPs, thereby confirming their formation. This optical signature is typically attributed to intrinsic band gap transitions of ZnO nanostructures and serves as a reliable indicator of nanoparticle synthesis. In addition to nanoparticle characterization, the UV spectrum of the *S. iscanderi* extract itself exhibited a distinct absorption peak around 320 nm. This peak corresponds to the electronic transitions commonly associated with phenolic compounds and flavonoids, which are known to play a pivotal role in the reduction and stabilization of metal ions during the green synthesis process. These findings not only validate the formation of ZnO-NPs but also highlight the biochemical composition of the extract, suggesting its dual function as both a reducing and capping agent in the biosynthetic pathway (Figure 3).

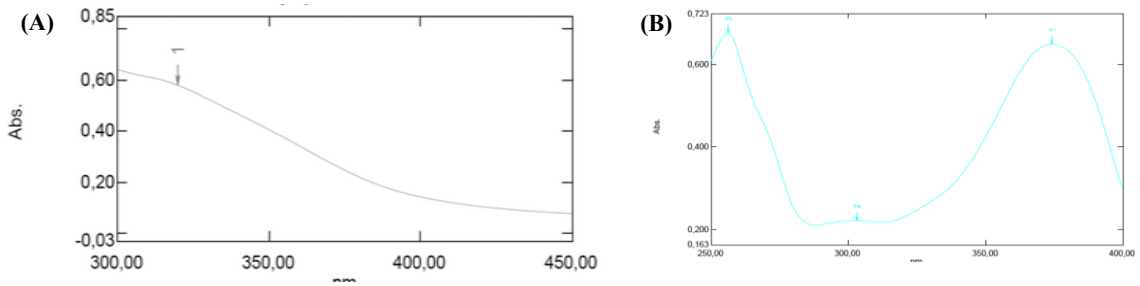

Figure 3. UV spectrum of the aqueous extract **(A)** and the substance containing ZnO-NPs **(B)**

3.3. Determination of Flavonoid Content by HPLC Analysis

Considering that *S. iscanderi* contains flavonoid compounds particularly luteolin, apigenin, quercetin, and rutin that participate in the formation of metal nanoparticles, a comparative chromatographic study was conducted to analyze the flavonoid content in the aqueous extract of *S. iscanderi* and the substance containing ZnO-NPs. Figures 4-7 present the HPLC chromatograms of extracts and their corresponding ZnO-NP-loaded forms, namely apigenin (Figure 4), quercetin (Figure 5), rutin (Figure 6), and luteolin (Figure 7), where (A) represents the pure extract and (B) the extract containing ZnO-NPs.

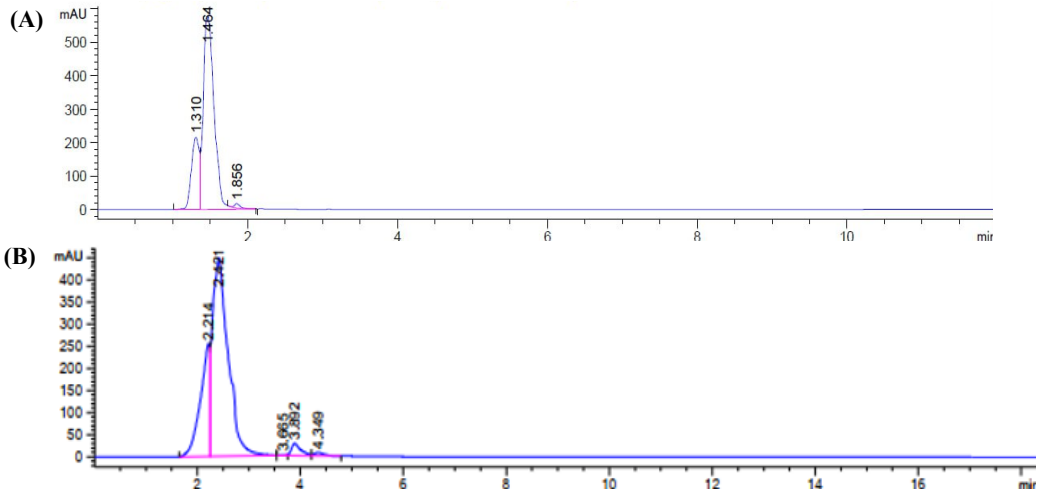

Figure 4. HPLC chromatogram of extract (apigenin) **(A)** and extract containing ZnO-NPs (apigenin) **(B)**

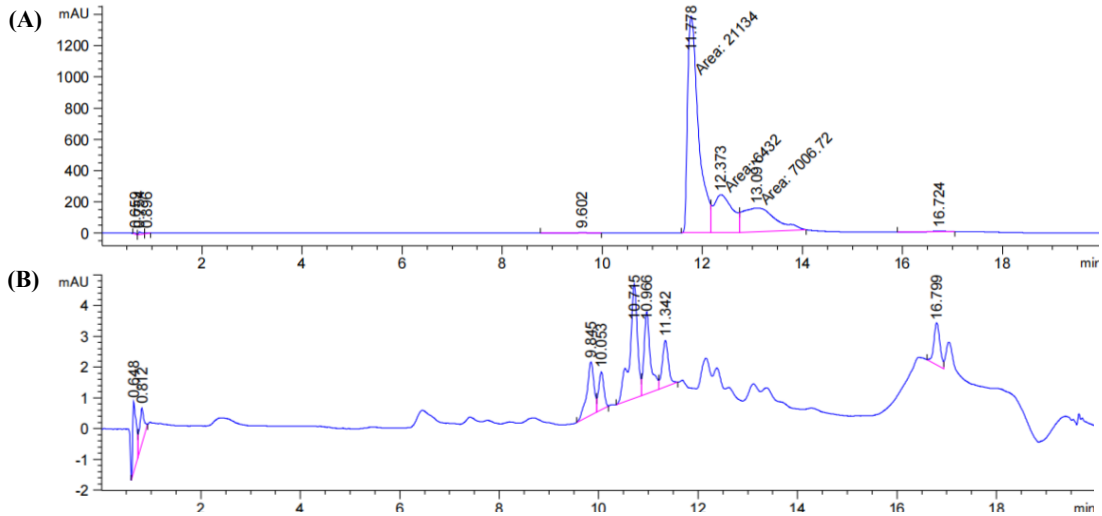

Figure 5. HPLC chromatogram of extract (quercetin) **(A)** and extract containing ZnO-NPs (quercetin) **(B)**

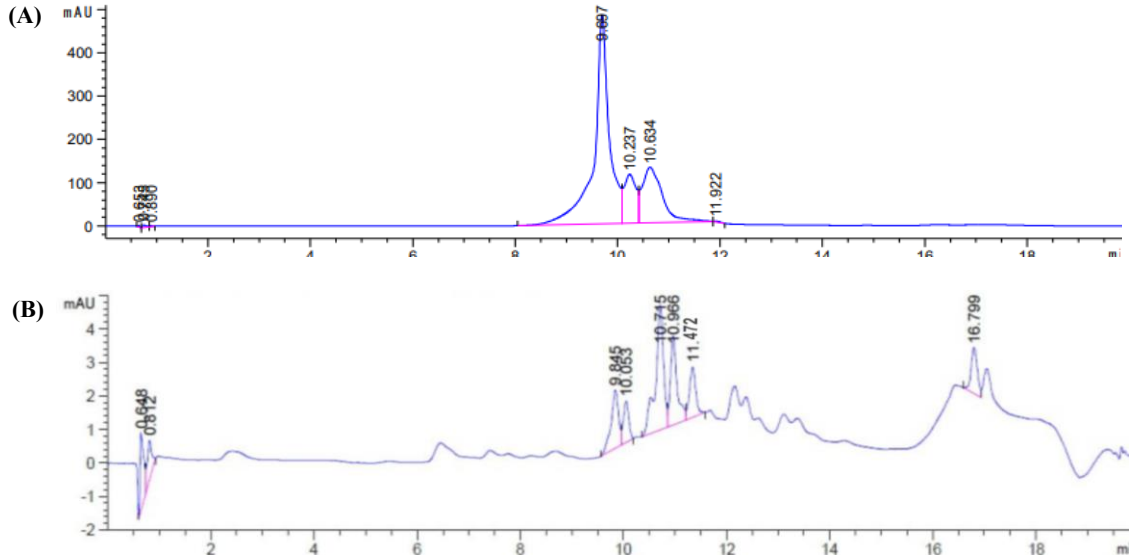

Figure 6. HPLC chromatogram of extract (rutin) **(A)** and extract containing ZnO-NPs (rutin) **(B)**

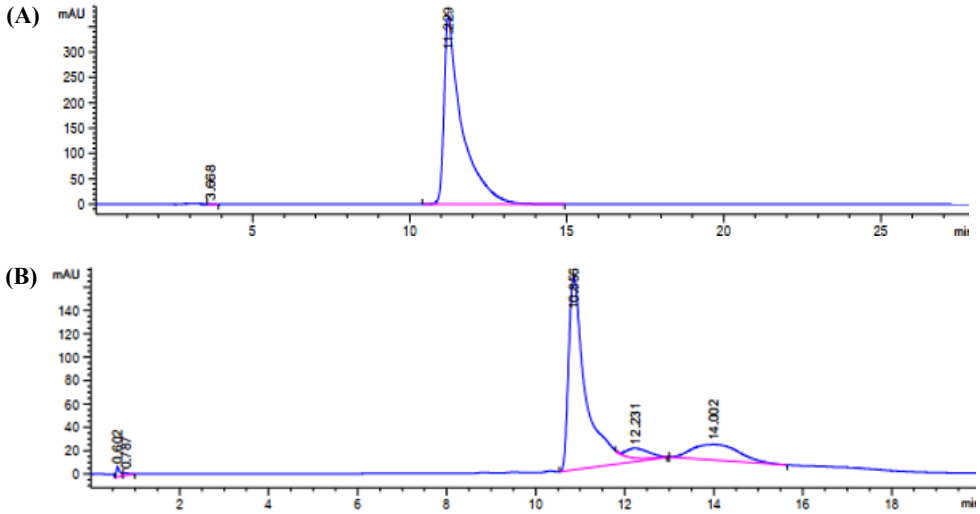

Figure 7. HPLC chromatogram of extract (luteolin) **(A)** and extract containing ZnO-NPs (luteolin) **(B)**

Initially, chromatograms of the flavonoid standards were recorded: quercetin at 11.77 min, rutin at 9.69 min, apigenin at 1.49 min and luteolin at 11.29 min. Subsequently, chromatograms were obtained for the solution of the original *S. iscanderi* extract and for the suspension of the *S. iscanderi* extract containing ZnO-NPs. The results of these analyses are shown in Figure 7. As evident from the presented chromatograms, peaks were observed at wavelengths of 269, 370, 357, and 350 nm, with retention times (min) corresponding to the presence of quercetin at 11.79 min, rutin at 9.84 min, apigenin at 1.47 min, and luteolin at 11.43 min. According to the analysis results, the content of flavonoids in the samples containing ZnO-NPs was reduced. A summary of the chromatographic analysis results is presented in Table 3.

Table 3. Quantitative content of selected flavonoids in *S. iscanderi* extract and the final substance

Flavonoid Standard	**Flavonoid Content, mg/g**	
	***S. iscanderi* Extract**	**Substance**
Apigenin	0.372	0.130
Quercetin	0.146	0.052
Rutin	0.242	0.062
Luteolin	0.133	0.101

3.4. Identification of Carbohydrates Involved in Nanoparticle Formation

Since *S. iscanderi* contains not only flavonoid compounds but also carbohydrates and proteins that may potentially participate in the formation of ZnO-NPs, a comparative chromatographic analysis of the aqueous extract of *S. iscanderi* and the resulting suspension containing ZnO-NPs was carried out to determine the carbohydrate content in the given samples. Standard chromatograms of carbohydrates were obtained, with retention times as follows: fructose 4.9±0.2 min, glucose 5.7±0.2 min, sucrose 10.4±0.2 min, and maltose 12.1±0.2 min (Figure 8). Subsequently, chromatograms of the aqueous extract of *S. iscanderi* were recorded, as well as chromatograms of the substance containing ZnO-NPs synthesized from this extract (Figure 9). The summarized data obtained from chromatographic analysis are presented in Table 4.

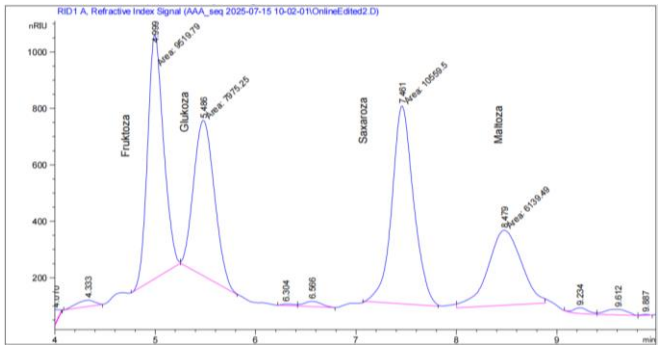

Figure 8. Chromatogram of carbohydrate standards: fructose, glucose, sucrose and maltose

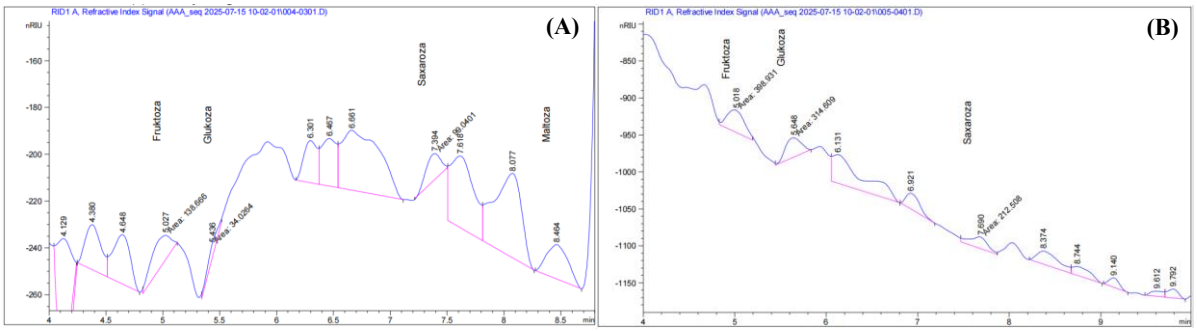

Figure 9. Chromatogram of extract (Carbohydrate analysis: fructose, glucose, sucrose, maltose) **(A)** and extract containing ZnO-NPs (Carbohydrate analysis: fructose, glucose, sucrose, maltose) (**B)**

Table 4. Quantitative content of selected carbohydrates in the extract and substance containing ZnO-NPs

Carbohydrates	Extract of *S. iscanderi*	Substance with ZnO-NPs
	Concentration, mg/g	
Fructose	0.059	0.17
Glucose	0.016	0.144
Sucrose	0.039	0.083
Maltose	0.101	0
Total	**0.215**	**0.397**

3.5. Amino Acid Profiling Before and After Nanoparticle Synthesis

For the identification of amino acid derivatives, the method of HPLC was employed. Chromatograms of the aqueous extract of *S. iscanderi*, as well as chromatograms of the sample containing ZnO-NPs formed in the extract (Figure 10), were obtained for this purpose.

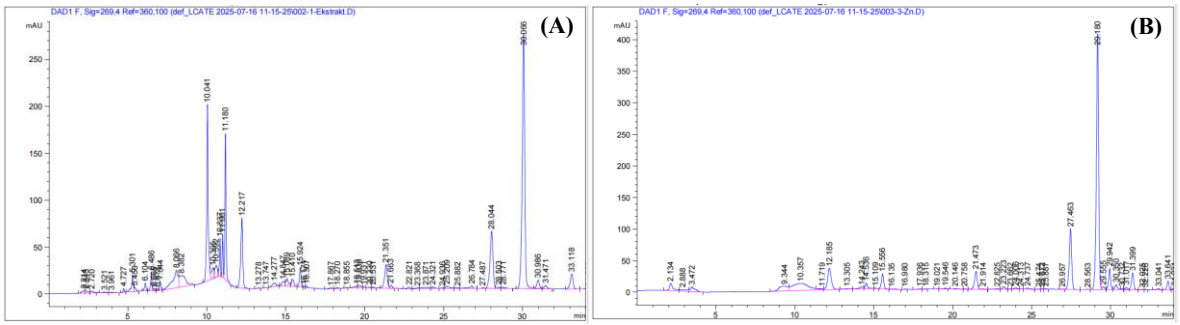

Figure 10. Chromatogram of extract **(A)** and extract containing ZnO-NPs (**B)**

Comparative data on the amino acid composition of *S. iscanderi* extract and the substance containing ZnO-NPs are presented in Table 5. Analysis of the data in the table shows the complete disappearance of a number of amino acids, such as aspartic acid, glutamic acid,

glycine, asparagine, cysteine, threonine, arginine, alanine, methionine, leucine, and lysine, which were detected in the original extract, in the substance containing ZnO-NPs. At the same time, an increase in the content of histidine in the substance was noted. In addition, a decrease in the quantitative content of such amino acids as glutamine, serine, tyrosine, valine, histidine, isoleucine, tryptophan, and phenylalanine was observed.

Table 5. Quantitative content of individual amino acids in extract and the substance containing ZnO-NPs

No	Amino Acid Name	*S. iscanderi* Extract	Substance with ZnO-NPs
		Concentration (mg/ml)	
1.	Aspartic acid	0.232	0.000
2.	Glutamic acid	0.070	0.000
3.	Serine	0.076	0.016
4.	Glycine	0.074	0.009
5.	Asparagine	0.075	0.000
6.	Glutamine	0.154	0.116
7.	Cysteine	0.106	0.000
8.	Threonine	0.584	0.000
9.	Arginine	0.179	0.005
10.	Alanine	0.056	0.044
11.	Proline	0.083	0.109
12.	Tyrosine	0.018	0.012
13.	Valine	0.247	0.016
14.	Methionine	0.034	0.025
15.	Histidine	0.080	0.178
16.	Isoleucine	0.034	0.029
17.	Leucine	0.021	0.031
18.	Tryptophan	0.030	0.007
19.	Phenylalanine	0.516	0.083
20.	Lysine	0.010	0.027
	Total	**2.678**	**0.706**

3.6. Proposed Mechanism of ZnO-NPs Formation Mediated by Plant Extract

Amino acids play a complex and multifunctional role in the process of biosynthesis of ZnO-NPs, ensuring both the initial stage of particle formation and their further stabilization. Due to the presence of various functional groups carboxyl, amino groups, and in some cases sulfhydryl amino acids can effectively interact with zinc ions (Zn^{2+}), forming coordination complexes. These complexes play a key role at the nucleation stage, contributing to the directed precipitation and crystallization of ZnO. Amino acids with polar side chains, such as aspartic and glutamic acids, are of particular importance, as they can stabilize the forming nanoparticles by forming hydrogen bonds and electrostatic interactions with ions on the particle surface (Liu et al., 2010; Singh et al., 2018). In addition, amino acids containing amino groups (for example, arginine, lysine) take part in the spatial stabilization of nanostructures, preventing particle aggregation by forming a strong protective shell. Some amino acids, such as cysteine and methionine, due to the presence of thiol or thioether groups, can not only stabilize the surface of nanoparticles, but also influence their growth, morphology, and crystal structure (Sandmann et al., 2015). In turn, non-polar amino acids (alanine, proline) provide additional stabilization of the particles through hydrophobic interactions, especially in aqueous medium, promoting the formation of more homogeneous and stable nanostructures. Thus, amino acids act as natural agents simultaneously influencing the mechanism of nanoparticle formation, their size, shape, and stability. Their participation in the process of ZnO-NPs biosynthesis makes it possible to obtain functional nanomaterials with controlled parameters without the use of toxic chemical reagents, which is especially relevant for biomedical and pharmaceutical applications (Mahakal et al., 2023).

The results of the conducted study confirm the high efficiency of the plant extract *S. iscanderi* as a biogenic agent in the synthesis of ZnO-NPs via the "green" synthesis method. It was established that the biochemical compounds present in the extract, such as flavonoids, carbohydrates, and amino acids, actively participate in the reduction and stabilization processes of nanostructures. Amino acids play a particularly important role, as they are capable of forming coordination complexes with zinc ions due to their carboxyl, amino, and other functional groups, thereby ensuring directed nanoparticle precipitation and stabilization (Molina et al., 2011). The decrease in the content of certain amino acids such as aspartic acid, glutamic acid, serine, and others in the substance with nanoparticles compared to the initial extract may indicate their active involvement in the reaction. Similarly, the reduction in the concentration of flavonoids (apigenin, quercetin, rutin, luteolin) confirms their participation in the reduction and stabilization of nanoparticles. This is consistent with the literature data emphasizing the role of flavonoids as antioxidants and natural stabilizers (Sandra and Martins, 2021).

Nevertheless, an interesting observation was the increase in the content of certain amino acids in the suspension containing ZnO-NPs compared to the initial aqueous extract of *S. iscanderi*. The most significant increase in concentration was recorded for amino acids such as proline, tyrosine, histidine, and leucine. This may be due to several factors. First, during the synthesis of nanoparticles, partial hydrolytic cleavage of proteins or peptides contained in the plant extract may occur under the influence of temperature, pH, and the presence of metal ions. This, in turn, leads to the release of free amino acids, which is detected during analytical determination. Second, the release of amino acids from complex glycoprotein or phenolic conjugates, which in the original extract were in bound, insoluble, or inactive forms, is possible. During biosynthesis, these compounds may undergo modification, releasing amino acids in a soluble form (Singh et al., 2018). Third, it is not excluded that part of the amino acids may have been desorbed from the surface of the nanoparticles due to a change in the medium conditions (for example, upon addition of NaOH), which could also contribute to the increase in their concentration in the free phase. Thus, the increase in the content of individual amino acids after the synthesis of nanoparticles can be considered a result of the breakdown of macromolecules and the activation of the previously bound amino acid pool, which does not contradict known mechanisms of plant-based nanoparticle biosynthesis.

It has been established that an increase in the extraction temperature contributes to more complete flavonoid extraction, which directly affects the efficiency and rate of nanoparticle biosynthesis (Buniyamin et al., 2024). The fastest nanoparticle formation was observed at a temperature of 50°C and an extract-to-zinc acetate ratio of 3:2, which can be considered the optimal synthesis conditions. FTIR spectroscopy revealed characteristic absorption bands indicating the involvement of functional groups of phenolic compounds, proteins, and carbohydrates in the formation of nanostructures. UV spectra demonstrated the successful formation of ZnO-NPs with a characteristic absorption maximum at 370 nm, consistent with the literature data (Haji et al., 2025). Moreover, this study confirms the involvement of carbohydrates such as fructose, glucose, and sucrose in the process of nanoparticle formation, as evidenced by their increased content in the final substance. Plant-derived sugars present in the extracts play a significant role in the biogenesis of metallic nanoparticles. Among them, monosaccharides such as glucose, which possesses a linear structure with an aldehyde group, can directly act as reducing agents and initiate nanoparticle formation. Ketoses, including fructose, exhibit reducing activity only after tautomerization accompanied by a transition from the ketone to the aldehyde form, which limits their reducing capacity due to kinetic factors (Makarov et al., 2014).

The reducing potential of disaccharides and polysaccharides is largely determined by the ability of their monomeric units to adopt an open-chain structure, allowing access to functional

groups capable of reducing metal ions. For example, disaccharides such as lactose and maltose display reducing activity, whereas sucrose due to the glycosidic bond between glucose and fructose, which prevents ring opening does not exhibit such activity. However, when using stronger acidic reducing agents, such as tetrachloroauric or tetrachloroplatinic acid, hydrolysis of sucrose is possible, leading to the formation of free monomers capable of participating in nanoparticle synthesis (Panigrahi et al., 2004). It is assumed that the mechanism of metal ion reduction involves oxidation of the sugar's aldehyde group to a carboxyl group through nucleophilic attack by hydroxide ions, which in turn leads to the formation of metallic nanoparticles. A similar mechanism has been described for the biosynthesis of nanoparticles using plant extracts such as *Schisandra* extract (Shankar et al., 2003).

Thus, the use of a "green" synthesis method employing *S. iscanderi* extract enables the production of stable ZnO-NPs with high efficiency and potential for pharmaceutical and biomedical applications. The conducted study highlights the promise of biosynthesis as a sustainable, scalable, and environmentally safe alternative to traditional physico-chemical nanoparticle synthesis methods.

4. CONCLUSION

The results of this study show that the aqueous extract of *S. iscanderi* can be successfully used as a natural agent with both reducing and stabilizing properties for the green synthesis of ZnO-NPs. The biologically active compounds in the extract flavonoids, amino acids, and carbohydrates play a central role in the reduction of zinc ions and the formation of nanostructures. FTIR and UV-Vis spectroscopy confirmed that ZnO-NPs were synthesized and that functional groups of natural compounds are involved in their stabilization. A comparative chemical analysis before and after synthesis showed a decrease in several amino acids and flavonoids, proving that they were consumed in nanoparticle formation. At the same time, some amino acids increased in concentration, most likely because proteins were hydrolyzed and released bound amino acids into the solution. The results also demonstrated that monosaccharides and disaccharides take part in the reduction process. This is explained by their ability to adopt an open-chain structure and show reducing activity. The best conditions for ZnO-NP synthesis were observed at 50°C with an extract-to-zinc acetate ratio of 3:2. These optimized parameters make the process efficient and reproducible. Overall, the findings highlight S. iscanderi as a promising plant-based resource for eco-friendly, scalable, and cost-effective nanoparticle synthesis. Such nanostructures have wide potential for applications in pharmaceutical, agricultural, and biomedical fields. Future research should investigate the biological properties of the synthesized ZnO-NPs, improve large-scale production methods, and explore their practical use in medicine and biotechnology.

Conflict of Interest
The authors declare that they have no conflicts of interest.

Author Contribution Statement
Shamansur Sagdullayev and Iroda Shermatova: Conceptualisation and design; Iroda Shermatova, Dilobar Tayirova, Zakirova Rukhsona: Methodology and data analysis; Azizakhon Khusniddinova, Shamansur Sagdullayev, Iroda Shermatova: Writing, review and editing.

Data Availability Statement
The authors confirm that the data supporting the findings of this study are available within the article. No additional datasets were generated or analyzed during the current study.

Acknowledgement
The authors gratefully acknowledge the Agency for Innovative Development of the Republic of Uzbekistan for supporting the experimental part of this study within the framework of the "Academic Mobility" grant.

REFERENCES

Akşit H, Gergin Ö. (2025). Synthesis and antimicrobial evaluation of silver nanoparticles mediated by *Alchemilla erzincanensis*. *Journal of Science and Mathematics Letters*, 13(2), 48-56. doi:10.37134/jsml.vol13.2.4.2025

Al-darwesh MY, Ibrahim SS, Mohammed MA. (2024). A review on plant extract mediated green synthesis of zinc oxide nanoparticles and their biomedical applications. *Results in Chemistry*, 7, 101368. doi:10.1016/j.rechem.2024.101368

Azam A, Ahmed AS, Oves M, Khan MS, Habib SS, Memic A. (2012). Antimicrobial activity of metal oxide nanoparticles against gram-positive and gram-negative bacteria: a comparative study. *International Journal of Nanomedicine*, 6003-6009. doi:10.2147/IJN.S35347

Buniyamin I, Asli NA, Eswar KA, Syed Abd Kadir SAIA, Saiman A, Idorus MY, Mahmood MR, Khusaimi Z. (2024). Biosynthesis of Tin(IV) Oxide nanoparticles (SnO_2 NPs) via *Chromolaena odorata* leaves: The influence of heat on the extraction procedure. *Journal of Science and Mathematics Letters*, 12(2), 142-150. doi:10.37134/jsml.vol12.2.11.2024

Cohen SA, Strydom DJ. (1988). Amino acid analysis utilizing phenylisothiocyanate derivatives. *Analytical Biochemistry*, 174(1), 1-16. doi:10.1016/0003-2697(88)90512-x.

Haji BS, Barzinjy AA, Abbas AO, Kaygili O, Mousa MS. (2025). Green synthesis of ZnO nanoparticles using Citrullus lanatus fruit extract and their potential for microwave absorption. *Nano-Structures and Nano-Objects*, 43, 101502. doi:10.1016/j.nanoso.2025.101502

Javed R, Zia M, Naz S, Aisida SO, Ain NU, Ao Q. (2020). Role of capping agents in the application of nanoparticles in biomedicine and environmental remediation: recent trends and future prospects. *Journal of Nanobiotechnology*, 18(1), 172. doi:10.1186/s12951-020-00704-4

Khan I, Saeed K, Khan I. (2019). Nanoparticles: Properties, applications and toxicities. *Arabian Journal of Chemistry*, 12(7), 908-931. doi:10.1016/j.arabjc.2017.05.011

Lithi IJ, Ahmed Nakib KI, Chowdhury AMS, Sahadat Hossain M. (2025). A review on the green synthesis of metal (Ag, Cu, and Au) and metal oxide (ZnO, MgO, Co_3O_4 and TiO_2) nanoparticles using plant extracts for developing antimicrobial properties. *Nanoscale Advances*, 7(9), 2446-2473. doi:10.1039/d5na00037h

Liu H, Huang B, Wang Z, Qin X, Zhang X, Wei J, Dai Y, Wang P, Whangbo MH. (2010). Amino acid-assisted synthesis of ZnO twin-prisms and functional group's influence on their morphologies. *Journal of Alloys and Compounds*, 507(1), 326-330. doi: 10.1016/j.jallcom.2010.07.192

Mahakal S, Pathan HM, Prasad M, Rondiya S, Patole SP, Jadkar SR. (2023). Modification in toxicity of l-histidine-incorporated ZnO nanoparticles toward *Escherichia coli*. *ACS Omega*, 8(38), 34354-34363. doi:10.1021/acsomega.3c01183

Makarov VV, Love AJ, Sinitsyna OV, Makarova SS, Yaminsky IV, Taliansky ME, Kalinina NO. (2014). "Green" nanotechnologies: synthesis of metal nanoparticles using plants. *Acta Naturae*, 6(1), 35-44.

Molina R, Al-Salama Y, Jurkschat K, Dobson PJ, Thompson IP. (2011). Potential environmental influence of amino acids on the behavior of ZnO nanoparticles. *Chemosphere*, 83(4), 545-551. doi:10.1016/j.chemosphere.2010.12.020

Panigrahi S, Kundu S, Ghosh SK, Nath S, Pal T. (2004). General method of synthesis for metal nanoparticles. *Journal of Nanoparticle Research*, 6, 411-414. doi:10.1007/s11051-004-6575-2

Rajiv P, Rajeshwari S, Venckatesh R. (2013). Bio-Fabrication of zinc oxide nanoparticles using leaf extract of *Parthenium hysterophorus* L. and its size-dependent antifungal activity against plant fungal pathogens. *Spectrochimica Acta Part A: Molecular and Biomolecular Spectroscopy*, 112, 384-387. doi:10.1016/j.saa.2013.04.072

Ramesh M, Anbuvannan M, Viruthagiri G. (2015). Green synthesis of ZnO nanoparticles using Solanum nigrum leaf extract and their antibacterial activity. *Spectrochimica Acta Part A: Molecular and Biomolecular Spectroscopy*, 136, 864-870. doi:10.1016/j.saa.2014.09.105

Sandmann A, Kompch A, Mackert V, Liebscher CH, Winterer M. (2015). Interaction of L-cysteine with ZnO: structure, surface chemistry, and optical properties. *Langmuir*, 31(21), 5701-5711. doi:10.1021/la504968m

Sandra R, Martins L. (2021). Antioxidant activity as an indicator of the efficiency of plant extract-mediated synthesis of zinc oxide nanoparticles. *Antioxidants*, 12(4), 784. doi:10.3390/antiox12040784

Shankar SS, Ahmad A, Pasricha R, Sastry M. (2003). Bioreduction of chloroaurate ions by geranium leaves and its endophytic fungus yields gold nanoparticles of different shapes. *Journal of Materials Chemistry*, 13(7), 1822-1826. doi:10.1039/B303808B

Shermatova IB, Rizayev KS. (2025). Technology of obtaining and studying the process of green synthesis with gold nanoparticles. *Journal of Neonatal Surgery*, 14(22), 529-534.

Singh B, Moudgil L, Singh G, Kaura A. (2018). Amino acid-assisted synthesis of zinc oxide nanostructures. *In AIP Conference Proceedings*, 1953(1), 030204. doi:10.1063/1.5032539

Singh P, Dutta T, Kim KH, Rawat M, Samddar P, Kumar P. (2018). 'Green' synthesis of metals and their oxide nanoparticles: applications for environmental remediation. *Journal of Nanobiotechnology*, 16(1), 84. doi:10.1186/s12951-018-0408-4

Singh P, Hamid M, Singh H, Srivastava S. (2022). Applications of green synthesis of nanoparticles using microorganisms in food and dairy products: review. *Processes*, 13(5), 1560. doi:10.3390/pr13051560